


Origin of off-stoichiometry and electrical benignity at the grain boundaries in CuInSe_2 : A first-principles study

Cite as: J. Appl. Phys. 128, 145702 (2020); doi: 10.1063/5.0018397

Submitted: 14 June 2020 · Accepted: 24 September 2020 ·

Published Online: 12 October 2020



Guo-Jun Zhu,¹ Ji-Hui Yang,^{1,a)}  and Xin-Gao Gong^{1,2,a)}

AFFILIATIONS

¹Department of Physics, Key Laboratory for Computational Science (MOE), State Key Laboratory of Surface Physics, Fudan University, Shanghai 200433, China

²Collaborative Innovation Center of Advanced Microstructures, Nanjing 210093, Jiangsu, China

^{a)}Authors to whom correspondence should be addressed: jhyang04@fudan.edu.cn and xggong@fudan.edu.cn

ABSTRACT

Grain boundaries (GBs) in polycrystalline CuInSe_2 are of both fundamental interest and technological significance for photovoltaic applications. However, the atomic composition and the exact roles of the GBs in CuInSe_2 are still unclear despite a large off-stoichiometry around the GBs being reported. In this work, based on first-principles calculations and using $\Sigma 3(114)$ GB as an example, we show that the GB acts as a sink of defects, leading to defect segregations and off-stoichiometry. Furthermore, depending on the chemical potential conditions, different point defects dominate the different segregations. Under common experimental conditions with In rich and Cu poor, we find that the most dominant defect at the GBs is the antisite defect In_{Cu} . Our studies show that the existence of In_{Cu} can eliminate defect states in the bandgap and thus suppress recombination of photo-generated electron-hole pairs, making the GB electrically benign. To enhance the formation of In_{Cu} , we propose an optimal region of chemical potential to realize In segregation and Cu depletion at the GB. Our work thus provides useful insights and understandings for further improvement of CISE polycrystalline solar cells.

Published under license by AIP Publishing. <https://doi.org/10.1063/5.0018397>

INTRODUCTION

Optoelectronic devices such as photovoltaic solar cells often necessitate monocrystalline active materials without grain boundaries (GBs) because monocrystalline solar cells usually exhibit better performance compared to their polycrystalline counterparts.¹ For example, commercial panel solar cells based on monocrystalline silicon have reached an energy conversion efficiency of up to 26.3% compared to about 21.3% for those based on polycrystalline silicon. The relatively poor performance of polycrystalline solar cells is commonly explained by classical GB models, where chemical impurities and structural defects tend to segregate at GBs from the grain interior (GI) during growth and introduce deep in-gap states. These states often act as effective recombination centers for the optically generated electrons and holes, thus reducing photovoltaic energy conversion efficiency.^{1,2} Such GB models have successfully explained the low energy conversion efficiency in many solar cells.

Recently, multiple chalcogenides such as CuInSe_2 (CISE) and $\text{Cu}_2\text{ZnSnSe}_4$ (CZTSe) have shown great promise for the absorber layers in photovoltaic devices due to their low cost and high energy conversion efficiency.^{3,4} In contrast to classical GB models, GBs in CISE can benefit rather than reduce solar cell efficiencies. For example, polycrystalline CISE solar cells can achieve efficiencies of around 20%⁴ even without deliberate passivation, outperforming its best monocrystalline devices ($\sim 13\%$).⁵ To understand the mechanism of GB benignity in CISE polycrystalline films, researchers have made tremendous research efforts in the past,^{6–8} and two main models have been proposed. In the first model, a potential barrier is created by GB, which repels majority carriers (holes)^{6,9–11} away from the GB area and benefits the photovoltaic effect. Experimentally, Hetzer *et al.*¹² performed nanoscale electrical characterization and found the local built-in potential near the GB of Cu(In,Ga)Se_2 (CIGS) thin films. They reported a work function decrease of up to 480 meV and massive ($\sim 50\%$) loss of Cu

atoms at GB interfaces, leading to a valence band offset, which repels holes from the GB. Theoretically, calculations show that an energetic barrier arises from reduced p-d repulsion due to Cu-vacancy reconstruction,¹¹ which repels holes into the GI from the GB. In the second model, GBs play a similar role as that in the classical models, where GBs act as the sink of defects. However, large atomic relaxation induced by defects at GBs eliminates deep levels created by the GB interface and thus GBs become invalid recombination centers.¹³ Evidence is given by scanning tunneling spectroscopy¹⁴ that the density of deep level defects is reduced in the GB region more than in the GI region. Meanwhile, defects in the GB region are found electrically benign and not harmful to solar cell performance based on first-principles calculations.¹⁵

To reveal the exact role of GBs, it is of great importance to know the atomic composition information at the GBs. According to experimental results, the chemical composition mismatch is very serious near GBs of CIGS. For example, a Cu deficient region near GBs was identified by several different experimental methods.^{16–18} Combination of techniques including atomic force microscopy (AFM), scanning tunneling microscopy (STM), and transmission electron microscopy (TEM) showed Cu decreasing and In increasing within a few nm region around the GBs.¹⁹ However, Lei *et al.* reported that the GB in a sample deposited at 400 °C was In deficient and Se sufficient.²⁰ In general, different experiments with different growth conditions give different atomic compositions at GBs. Despite this, all experimental results have something in common; that is, off-stoichiometric composition at GBs in polycrystalline materials always exists, and if the Cu (In) signal is increased at the GBs, the In (Cu) signal will be reduced.^{17,21} Such a mismatch of components is quite similar to the defect properties in monocrystalline CIGS,²² in which the off-stoichiometry of In depletion and Cu depletion is mainly induced by the point defects V_{Cu} and In_{Cu} through forming ordered defects $In_{Cu}^{2+} + 2V_{Cu}^{-}$. Such ordered defects are also helpful to suppress relatively deep in-gap levels of In_{Cu}^{2+} and improve solar cell efficiencies as revealed by several theoretical works.^{8,22} Apparently, the off-stoichiometry in the bulk is not fully in agreement with experimental results at the GBs, and how the chemical composition mismatch near GBs arises and affects photovoltaic conversion efficiency is still unclarified, which makes the debate on the roles of GBs in CIGS unsettled.

In order to settle the debate on the roles of GBs and study the influence of the off-stoichiometric composition, we report the first-principles studies of GB structures with a slab model in polycrystalline CIGS. We use the $\Sigma 3(114)$ GB as an example in this study since this GB has been experimentally observed in zinc blende semiconductors^{22,23} and has a good research foundation.^{23,24} To study the atomic composition effects at GBs, we consider four kinds of point defects with their positions varying from the GI to the GB in our slab model. We find that the GB acts as a sink of defects because defects always have lower formation energies near the GB. The point defect formation energy dependence on the chemical potential conditions shows that the dominant defects can vary from In_{Cu} at the In-rich condition to V_{Cu} at the Cu-poor condition and then to Cu_{In} at the In-poor condition, thus explaining the diverse experimental findings. In addition, we consider alloying O with Se at the GB by noticing that recently, experiments reported a high O concentration on Se sites around the GB.^{16,17} We find

that the above conclusions still hold, and the introduction of O can make In_{Cu} more stable than other defects, especially if the O concentration is high. We then study the effect of In_{Cu} through the electronic properties of the GBs. The results show that the In_{Cu} antisite can eliminate the in-gap defect states and thus suppress recombination of photo-generated electron-hole pairs, which would benefit the photovoltaic performance of polycrystalline CIGS solar cells. To enhance the formation of In_{Cu} , we propose an optimal region based on the element chemical potential to realize In segregation and Cu depletion at the GB. Our study provides deep insights and understandings for the roles of off-stoichiometric composition at the grain boundaries, which would be useful for improving the efficiency of polycrystalline CIGS solar cells.

METHOD

The first-principles total-energy calculations are based on the density-functional theory using the Vienna *ab initio* simulation package (VASP).^{25,26} We use the standard frozen-core projector augmented-wave (PAW)^{27,28} method with 17, 13, and 6 valence electrons for Cu, In, and Se, respectively, to describe the interaction between valence electrons and ionic cores. A kinetic energy cutoff of 400 eV is used for plane-wave basis expansion. The general gradient approximation (GGA) prescribed by Perdew–Burke–Ernzerhof (PBE)²⁹ is used for the exchange–correlation potential. To correct the well-known bandgap errors, the commonly used plus U method is adopted. In this study, we use $U = 6$ eV on the cation d orbital.³⁰ To construct an accurate GB model without built-in electric fields, we build a slab model with a vacuum thickness of 20 Å, which contains only one GB. For the Brillouin zone sampling, the reciprocal space is presented by the Monkhorst–Pack special³¹ k-points method with a $2 \times 2 \times 1$ mesh for geometry relaxation and a $5 \times 5 \times 1$ mesh for static calculations. The convergence criteria are set to 1×10^{-6} eV and 0.01 eV/Å for total energies and Hellmann–Feynman forces on atoms, respectively.

The point defect formation energy ΔH_f in polycrystalline CIGS is defined as

$$\Delta H_f = \Delta E + n_{Cu}\mu_{Cu} + n_{In}\mu_{In} + n_{Se}\mu_{Se} + n_O\mu_O, \quad (1)$$

where

$$\Delta E = E(\text{defect}_{GB}) - E(\text{Host}_{GB}) + n_{Cu}\mu_{Cu}^0 + n_{In}\mu_{In}^0 + n_{Se}\mu_{Se}^0 + n_O\mu_O^0. \quad (2)$$

Here, $E(\text{Host}_{GB})$ is the total energy of polycrystalline CIGS without point defects, which is set as the reference; $E(\text{defect}_{GB})$ is the total energy of the defective polycrystalline CIGS; n_{Cu} , n_{In} , n_{Se} , and n_O are the number changes of Cu, In, Se, and O atoms when forming defective GB; and μ_{Cu} , μ_{In} , μ_{Se} , and μ_O are the chemical potentials of Cu, In, Se, and O, respectively, which are referenced to the total energies of stable elemental phases, μ_{Cu}^0 , μ_{In}^0 , μ_{Se}^0 , and μ_O^0 , respectively. Here, we choose face-centered cubic copper, body-centered cubic indium, Se_{64} , and oxygen molecules as the stable reference phases for Cu, In, Se, and O, respectively.

RESULTS AND DISCUSSIONS

Figure 1(a) shows our structural model for the $\Sigma 3(114)$ GB where we have adopted a slab model with only one GB core. To avoid interactions between periodic cells, a lattice with $a = 8.30$ Å, $b = 11.01$ Å, $c = 90$ Å, and $\gamma = 67.83^\circ$ is used, which contains 57 Cu atoms, 57 In atoms, 114 Se atoms, and 16 pseudo-hydrogen atoms. The upper and bottom four atomic layers in Fig. 1(a) are fixed to simulate the CISe bulk phase during structural relaxation. An enlarged view of the GB interface is given in Fig. 1(b) with the atoms near the GB labeled. After full relaxation, one weak bond between Se4 and Se4' [in Fig. 1(b)] is formed with a bond length of

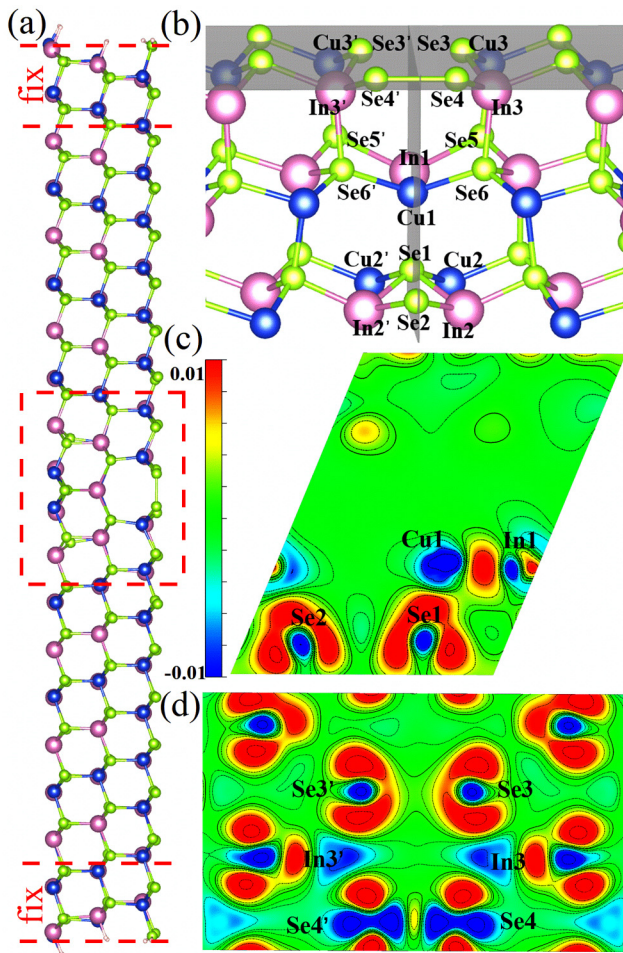


FIG. 1. Structure and charge information at the GB area. (a) Slab model of the $\Sigma 3(114)$ GB. The two surfaces are passivated with pseudo-H atoms. Green, blue, and purple balls are Se, Cu, and In, respectively. (b) The enlarged view of the local atomic structures near the GB core. (c) The charge transfer in the perpendicular plane of (b). (d) The charge transfer in the horizontal plane of (b). The charge transfer is calculated by $\rho = \rho(\text{GB}) - \rho(\text{In}_{\text{left}}) - \rho(\text{Cu}_{\text{left}}) - \rho(\text{Se}_{\text{left}}) - \rho(\text{In}_{\text{right}}) - \rho(\text{Cu}_{\text{right}}) - \rho(\text{Se}_{\text{right}})$. Note that the GB acts as a hole-accumulating state.

2.50 Å. At the same time, In1 and Cu1 form a strong bond with their distance shortened from 4.15 Å to 2.65 Å, as evidenced from the charge transfer in Figs. 1(c) and 1(d). However, for Se3 and Se3', they have a dangling bond with 0.25 electrons missing due to the two broken Cu–Se bond. Such dangling bonds make the whole GB act as a hole-accumulating state. Consequently, additional electrons, i.e., provided by defects, are expected to stabilize the GB structure.

To identify which defects are easily attracted to the GB, we first consider the formation energies of intrinsic defects by placing them at different distances from the GB. We consider four kinds of possible point defects including V_{Cu} , V_{In} , Cu_{In} , and In_{Cu} ,^{22,32} where V_{α} denotes a vacancy of atom α and α_{β} denotes an antisite of atom α on site β . The relative formation energies of these point defects at different distances from the GB are shown in Fig. 2. While the formation energies of point defects in the GI (far from the GB interface) are very close to those in the bulk,²² we find that the point defects near the GB interface have much smaller formation energies. Our calculations thus indicate that the point defects in polycrystalline CISe tend to segregate at the GB, in agreement with many experimental results.^{17,18,21} In this situation, the defects in the GI will move to the GB interface during the synthesis process, resulting in a purer grain structure, which is beneficial for improving the photovoltaic conversion efficiency.

Next, we consider the effects of the atomic chemical potentials on the defect formation energies and identify what defects are most possibly formed at the GB. To make sure CISe stabilize under equilibrium growth conditions, the atomic chemical potentials need to satisfy certain conditions. For example, to be in equilibrium with the elemental components, they should satisfy

$$\mu_{\text{Cu}} + \mu_{\text{In}} + 2\mu_{\text{Se}} = \Delta H_f(\text{CuInSe}_2) = -2.192 \text{ eV}, \quad (3)$$

where $\Delta H_f(\text{CuInSe}_2)$ is the formation enthalpy of the CISe. To avoid the formation of the secondary phases such as CuS, Cu_2S , InS , In_2S , and In_2Se_3 , the following relations must be satisfied:

$$\mu_{\text{Cu}} + \mu_{\text{Se}} < \Delta H_f(\text{CuSe}) = -0.378 \text{ eV}, \quad (4)$$

$$\mu_{\text{Cu}_2} + \mu_{\text{Se}} < \Delta H_f(\text{Cu}_2\text{Se}) = -0.678 \text{ eV}, \quad (5)$$

$$\mu_{\text{In}} + \mu_{\text{Se}} < \Delta H_f(\text{InSe}) = -1.167 \text{ eV}, \quad (6)$$

$$\mu_{\text{In}_2} + \mu_{\text{Se}} < \Delta H_f(\text{In}_2\text{Se}) = -0.830 \text{ eV}, \quad (7)$$

$$2\mu_{\text{In}} + 3\mu_{\text{Se}} < \Delta H_f(\text{In}_2\text{Se}_3) = -2.902 \text{ eV}, \quad (8)$$

$$\mu_{\text{Cu}} + 5\mu_{\text{In}} + 8\mu_{\text{Se}} < \Delta H_f(\text{CuIn}_5\text{Se}_8) = -9.086 \text{ eV}, \quad (9)$$

where $\Delta H_f(\text{CuSe})$, $\Delta H_f(\text{Cu}_2\text{Se})$, $\Delta H_f(\text{InSe})$, $\Delta H_f(\text{In}_2\text{Se})$, $\Delta H_f(\text{In}_2\text{Se}_3)$, and $\Delta H_f(\text{CuIn}_5\text{Se}_8)$ are the calculated formation enthalpies of binary and ternary compounds. Under these constraints, the chemical potentials of Cu and In that can stabilize CISe are bound to a polygon in the two-dimensional (μ_{Cu} and μ_{In}) space, as shown in Fig. 3. We find that the region is not very large with the

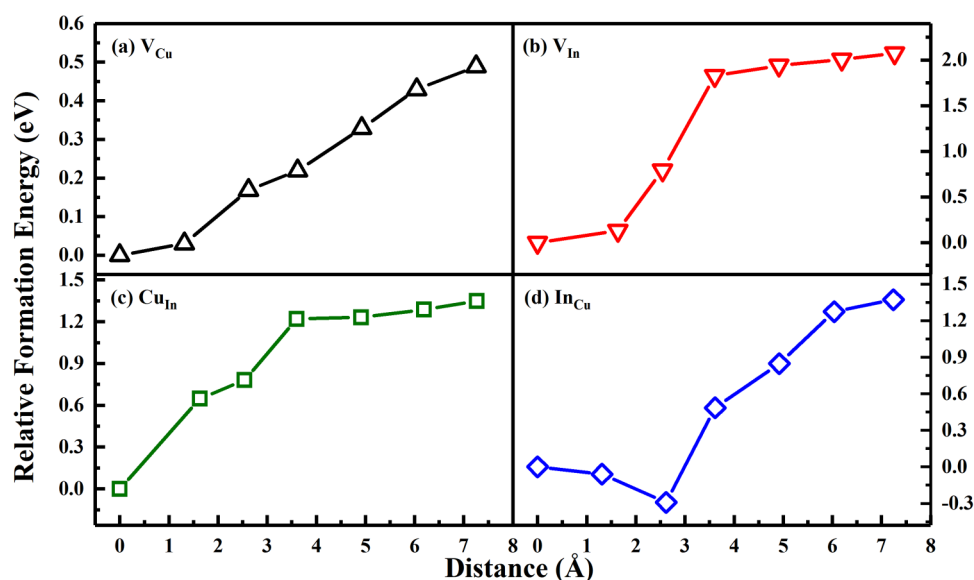


FIG. 2. The relative formation energies of four point defects at different distances from the GB core, including (a) V_{Cu} , (b) V_{In} , (c) Cu_{In} , and (d) In_{Cu} . The horizontal axis means the distance from the GB interface to the defect position. For each defect, we set the formation energy at the GB core as zero. Note that the formation energies near the GB interface are much lower than those in the GI.

chemical potentials of Cu and In being limited within 0.000–0.625 eV and –0.306 to 1.815 eV, respectively. Within this region, we chose five sidelines of the polygon in Fig. 3 to calculate the point defect formation energy dependence on the chemical potentials. The five vertices of the polygon represent different chemical potential conditions as the followings: point A represents Cu rich and In rich; points B, C, and D represent Cu and In relatively poor; and point E represents Cu rich and In poor. Different from the case in monocrystalline ClSe that the formation energies of V_{Cu} and Cu_{In} are

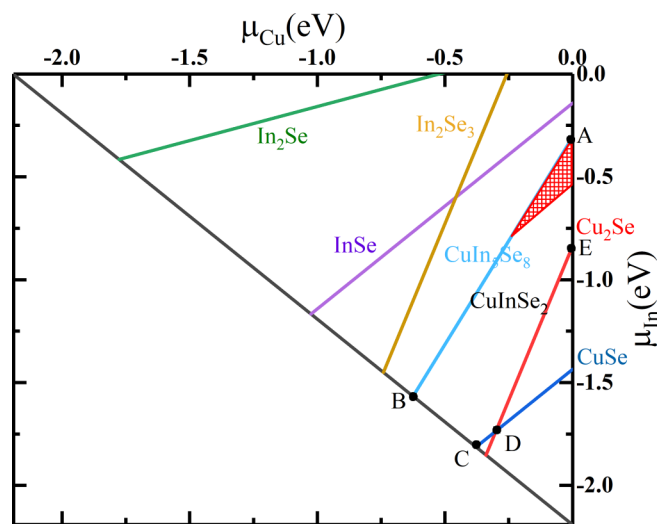


FIG. 3. The calculated region of chemical potentials to form stable ClSe. The red grid area indicates the chemical potential region that the formation energy of In_{Cu} is lower than that of Cu_{In} .

lower than that of In_{Cu} .²² In_{Cu} near the GB will have a lower formation energy in a certain chemical potential region. It can be seen in Fig. 4(a) that the dominant defects change from In_{Cu} to Cu_{In} and back to In_{Cu} along A–B–C–D–E–A lines. Accordingly, the atomic composition at the GB gradually changes from Cu depletion and In abundance to Cu abundance and In depletion, thus explaining diverse experimental measurements.

Besides the intrinsic defects, we also consider O-related defects as O is introduced in the experiments.^{16,17} Apparently, O is most likely to substitute Se sites. Here, we consider two cases. First, we consider the case with a low O concentration by replacing one Se atom at the GB area with one O atom (denoted as O_{Se-GB}). The most stable substitutional site is found to be Se3 with an energy gain of 2.801 eV referenced to the clean GB. In this case, the relative stabilities of intrinsic defects do not change, as shown in Fig. 4(b). The only difference is that the formation energies of all the intrinsic defects are slightly increased. This can be understood as follows. The O_{Se3} defect breaks the inversion symmetry of $\Sigma 3(114)$ GB and induces a large atomic distortion; i.e., the original distances of $d_{Se3-Cu3}$ ($d_{Se3'-Cu3'}$) and $d_{Se3-In3}$ ($d_{Se3'-In3'}$) are changed from 2.44 Å and 2.54 Å to 2.00 Å (d_{O-Cu3}) and 2.04 Å (d_{O-In3}), respectively. For the case of a high O concentration, we replace the Se3, Se3', Se4, and Se4' atoms by four O atoms (denoted as $4O_{Se-GB}$), and we find that the energy gain is 1.361 eV/defect in this case. Because the electronegativity of O is larger than Se, the length of O-metal bonds becomes shorter than that of Se-metal bonds. The consequence of O introduction is that the weak bonds of Se3–Se3' and Se4–Se4' will be broken, which means that the new GB with $4O_{Se}$ defects would like to attract more defects that can donate electrons and repel defects that are electron-deficient. Among our considered defects, In_{Cu} , In_i , and Cu_i can provide electrons; thus, their formation energies are expected to decrease, while other defects that cannot provide electrons are expected to have larger formation energies. Indeed, comparing with defect-free GB, our

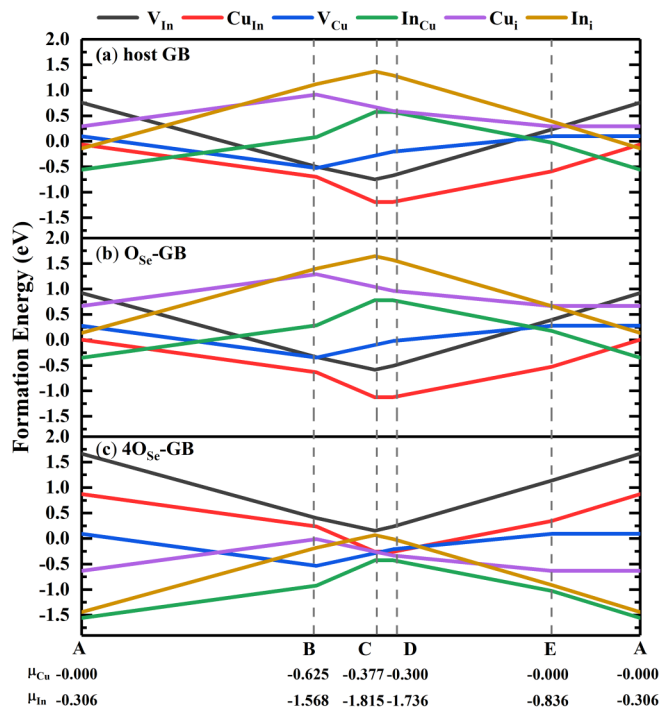


FIG. 4. The formation energies of intrinsic defects at the ClSe GB as a function of chemical potentials varying from A to B to C to D to E and back to A in Fig. 3. (a), (b), and (c) present the cases in the host GB, O_{Se} -GB, and $4O_{Se}$ -GB, respectively.

calculations show that the formation energies of In_{Cu} , Cu_i , and In_i are reduced by more than 1 eV, while the formation energies of V_{In} , V_{Cu} , and Cu_{In} are increased by nearly 1 eV in the $4O_{Se}$ -GB, as shown in Fig. 4(c). Moreover, under this situation, the most dominant intrinsic defect is always In_{Cu} throughout all the considered chemical potential intervals. This is because that In_i and Cu_i are expected to have larger defect formation energies than In_{Cu} as they will introduce large atomic distortions due to their large atomic sizes.

Based on the above discussion and considering the fact that ClSe is usually synthesized under In-rich and Cu-poor conditions, we can conclude that the most possible defect that can be formed at the GB is likely to be In_{Cu} , no matter whether O-related extrinsic defects are present or not. Our calculations thus provide a reasonable explanation of the Cu depletion and In segregation near the GB and demonstrate that the dangling bonds of Se3 and Se3' play the key roles in the defect formation process.

Now, we turn our focus to study how In_{Cu} at the GB affects the electronic properties of ClSe. It is clearly in Fig. 5(a) that the host GB has three in-gap states, which correspond to three unsaturated bonds including In1-Cu1, Se3-Se3', and Se4-Se4' as shown in Fig. 1. When In_{Cu} presents, the incipient In1-Cu1 wrong bond is broken, which eliminates one in-gap state and opens a bandgap, as shown in Fig. 5(b). Note that In_{Cu} in monocrystalline ClSe can induce a relatively deep level and thus is harmful. However, at the GB, In_{Cu} is actually helpful. When O_{Se} presents at the GB in addition to In_{Cu} , the Se3-Se3' wrong bond is replaced by the Se3'-O wrong bond. Since the electronegativity of O is much stronger than Se, the Se3'-O will be much weaker than Se3-Se3'. When this happens, the wrong bond introduced by

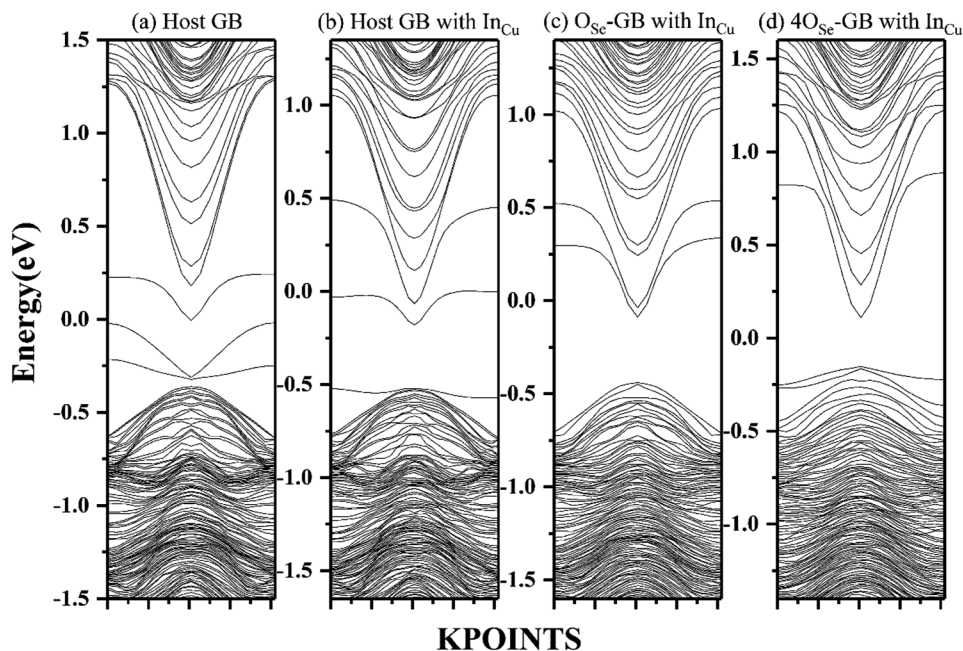


FIG. 5. Band structures of (a) the host GB, (b) the GB with the presence of In_{Cu} , (c) the O_{Se} -GB with the presence of In_{Cu} , and (d) the $4O_{Se}$ -GB with the presence of In_{Cu} .

Se3 and Se3' will be broken, and the GB will become more electrically benign, as seen in Fig. 5(c). Furthermore, when 4O_{Se} and In_{Cu} are present at the GB, all the in-gap states are eliminated, as shown in Fig. 5(d). This can be understood as that due to the large electronegativity of O, 4O_{Se} attracts more electrons from metallic atoms to O atoms and eliminates two in-gap states caused by dangling bonds of Se atoms. Moreover, the weak bond between In1 and Cu1 is broken with the distance increased from 2.65 Å to 4.00 Å. Consequently, all the three unsaturated bonds in the host GB are removed, and a relatively wide bandgap is opened. As In_{Cu} at the GB is of great importance to eliminate in-gap states and make the GB electrically benign, a high concentration of In_{Cu} is expected to help enhance photovoltaic energy conversion efficiency. To realize this, we give the optimal chemical potential conditions by considering the formation energies of In_{Cu}. As shown in Fig. 3, the red grid area indicates the chemical potential region that the formation energy of In_{Cu} is lower than that of Cu_{In}.

CONCLUSION

In conclusion, based on the first-principles density-functional theory, we have studied the defects at the $\Sigma 3(114)$ GB using the slab model in polycrystalline CISE. By providing the point defect formation energies, we show that the GB acts as a sink of defects because defects always have lower defect formation energies near GBs in our calculations. By considering the point defect formation energy dependence on the chemical potential conditions, we have explained the diverse experimental findings of elemental compositions at the GBs. Under common experimental conditions with In rich and Cu poor, we have concluded that the most dominant defect at the GBs is In_{Cu}, and the effect of In_{Cu} on the electronic properties of the GBs is to eliminate defect states in the bandgap and thus suppress recombination of photo-generated electron-hole pairs, which would benefit the photovoltaic performance of polycrystalline CISE solar cells. To further enhance the formation of In_{Cu}, we have proposed an optimal region to realize In segregation and Cu depletion at the GB. Our work is expected to help achieve higher photovoltaic energy conversion efficiency of CISE solar cells.

ACKNOWLEDGMENTS

This work was supported in part by the National Natural Science Foundation of China (NNSFC) (Grant No. 11974078), the Fudan Start-up funding (No. JIH1512034), and the Shanghai Sailing Program (No. 19YF1403100). Calculations are performed at the High-Performance Computing Center of Fudan University.

DATA AVAILABILITY

The data that support the findings of this study are available from the corresponding author upon reasonable request.

REFERENCES

- 1 M. A. Green, *J. Appl. Phys.* **80**, 1515 (1996).
- 2 P. P. Altermatt and G. Heiser, *J. Appl. Phys.* **91**, 4271 (2002).
- 3 P. Jackson, D. Hariskos, E. Lotter, S. Paetel, R. Wuerz, R. Menner, W. Wischmann, and M. Powalla, *Prog. Photovolt.* **19**, 894 (2011).
- 4 K. Ramanathan, M. A. Contreras, C. L. Perkins, S. Asher, F. S. Hasoon, J. Keane, D. Young, M. Romero, W. Metzger, R. Noufi, J. Ward, and A. Duda, *Prog. Photovolt.* **11**, 225 (2003).
- 5 Y. Yan, R. Noufi, and M. M. Al-Jassim, *Phys. Rev. Lett.* **96**, 205501 (2006).
- 6 R. Baier, C. Leendertz, D. Abou-Ras, M. C. Lux-Steiner, and S. Sadewasser, *Sol. Energy Mater. Sol. Cells* **130**, 124 (2014).
- 7 U. Rau, K. Taretto, and S. Siebentritt, *Appl. Phys. A* **96**, 221 (2009).
- 8 B. Huang, S. Chen, H. Deng, L. Wang, M. A. Contreras, R. Noufi, and S. Wei, *IEEE J. Photovolt.* **4**, 477 (2014).
- 9 C. S. Jiang, R. Noufi, J. A. AbuShama, K. Ramanathan, H. R. Moutinho, J. Pankow, and M. M. Al-Jassim, *Appl. Phys. Lett.* **84**, 3477 (2004).
- 10 C.-S. Jiang, M. Contreras, I. Repins, H. Moutinho, Y. Yan, M. Romero, L. Mansfield, R. Noufi, and M. Al-Jassim, *Appl. Phys. Lett.* **101**, 033903 (2012).
- 11 C. Persson and A. Zunger, *Phys. Rev. Lett.* **91**, 266401 (2003).
- 12 M. J. Hetzer, Y. M. Strzhemechny, M. Gao, M. A. Contreras, A. Zunger, and L. J. Brillson, *Appl. Phys. Lett.* **86**, 162105 (2005).
- 13 Y. Yan, C. S. Jiang, R. Noufi, S. H. Wei, H. R. Moutinho, and M. M. Al-Jassim, *Phys. Rev. Lett.* **99**, 235504 (2007).
- 14 H. Mönig, Y. Smith, R. Caballero, C. A. Kaufmann, I. Laueremann, M. Lux-Steiner, and S. Sadewasser, *Phys. Rev. Lett.* **105**, 116802 (2010).
- 15 W.-J. Yin, Y. Wu, R. Noufi, M. Al-Jassim, and Y. Yan, *Appl. Phys. Lett.* **102**, 193905 (2013).
- 16 D. Abou-Ras, B. Schaffer, M. Schaffer, S. S. Schmidt, R. Caballero, and T. Unold, *Phys. Rev. Lett.* **108**, 075502 (2012).
- 17 D. Abou-Ras, S. S. Schmidt, R. Caballero, T. Unold, H.-W. Schock, C. T. Koch, B. Schaffer, M. Schaffer, P.-P. Choi, and O. Cojocaru-Mirédin, *Adv. Energy Mater.* **2**, 992 (2012).
- 18 S. Siebentritt, S. Sadewasser, M. Wimmer, C. Leendertz, T. Eisenbarth, and M. Lux-Steiner, *Phys. Rev. Lett.* **97**, 146601 (2006).
- 19 W. Li, Y. Ma, S. Yang, J. Gong, S. Zhang, and X. Xiao, *Nano Energy* **33**, 157 (2017).
- 20 C. Lei, C. M. Li, A. Rockett, and I. M. Robertson, *J. Appl. Phys.* **101**, 024909 (2007).
- 21 D. Abou-Ras, S. S. Schmidt, N. Schäfer, J. Kavalakatt, T. Rissom, T. Unold, R. Mainz, A. Weber, T. Kirchartz, E. Simsek Sanli, P. A. van Aken, Q. M. Ramasse, H.-J. Kleebe, D. Azulay, I. Balberg, O. Millo, O. Cojocaru-Mirédin, D. Barragan-Yani, K. Albe, J. Haarstrich, and C. Ronning, *Phys. Status Solidi (RRL) – Rapid Research Letters* **10**, 363 (2016).
- 22 S. Zhang, S.-H. Wei, A. Zunger, and H. Katayama-Yoshida, *Phys. Rev. B* **57**, 9642 (1998).
- 23 Y. Yan, W.-J. Yin, Y. Wu, T. Shi, N. R. Paudel, C. Li, J. Poplawsky, Z. Wang, J. Moseley, H. Guthrey, H. Moutinho, S. J. Pennycook, and M. M. Al-Jassim, *J. Appl. Phys.* **117**, 112807 (2015).
- 24 H. Mirhosseini, J. Kiss, and C. Felser, *Phys. Rev. Appl.* **4**, 064005 (2015).
- 25 G. Kresse and J. Furthmüller, *Phys. Rev. B* **54**, 11169 (1996).
- 26 G. Kresse and J. Furthmüller, *Comput. Mater. Sci.* **6**, 15 (1996).
- 27 P. E. Blöchl, *Phys. Rev. B* **50**, 17953 (1994).
- 28 G. Kresse and D. Joubert, *Phys. Rev. B* **59**, 1758 (1999).
- 29 J. P. Perdew, K. Burke, and M. Ernzerhof, *Phys. Rev. Lett.* **77**, 3865 (1996).
- 30 C.-Y. Liu, Z.-M. Li, H.-Y. Gu, S.-Y. Chen, H. Xiang, and X.-G. Gong, *Adv. Energy Mater.* **7**, 1601457 (2017).
- 31 H. J. Monkhorst and J. D. Pack, *Phys. Rev. B* **13**, 5188 (1976).
- 32 S.-H. Wei and S. B. Zhang, *J. Phys. Chem. Solids* **66**, 1994 (2005).